IEEE International Magnetics Conference

May 4-8, 2014
Dresden, Germany

General Chairs
Ludwig Schultz
IFW Dresden and TU Dresden
l.schultz@ifw-dresden.de
Michael E. McHenry
Carnegie Mellon University
mm7g@andrew.cmu.edu

Conference Treasurer
Rudolf Schäfer
IFW Dresden
r.schaefer@ifw-dresden.de
Petru Andrei
Florida State University
pandrei@fsu.edu

Program Chairs
Nora Dempsey
CNRS - Institut NÉEL
nora.dempsey@grenoble.cnrs.fr
Russell Cowburn
University of Cambridge
rpc12@cam.ac.uk
Zbigniew Celinski
University of Colorado
zcelinsk@uccs.edu

Publication Chair
Oliver Gutfleisch
Technische Universität Darmstadt
gutfleisch@fm.tu-darmstadt.de

Exhibits Chair
Giselher Herzer
Vacuumschmelze Hanau
gherzer@gmail.com

Local Chairs
Heike Schlörb
IFW Dresden
h.schloerb@ifw-dresden.de
Jürgen Fassbender
Helmholtz-Zentrum Dresden-Rossendorf
j.fassbender@hzdr.de

Conference & Exhibit Management
CMD Congress Management GmbH Dresden
Desdemona Bock
info@cmd-congress.de

Student Travel Coordinator
Matthew J. Carey
Samsung New Memory Technologies, San Jose
M.Carey@ssi.samsung.com

Student Awards
Mingzhong Wu
Colorado State University, Fort Collins
mwu@lamar.colostate.edu

IEEE Representative
Massimo Pasquale
INRIM Torino
mpas@ieee.org

Conference Topics

Spin electronics • Magnetic recording • Life sciences • Sensors, MEMS, RF materials & devices • Motors, generators, transformers & power devices • Magnetic thin films & nanostructures • Functional magnetic materials • Soft magnetic materials • Permanent magnet materials • Modeling & computational magnetism • Fundamental properties & interdisciplinary topics • Microscopy, imaging & characterization

Deadlines

- Invited Presentation and Symposia Nominations: *November 17, 2013*
- Digest Submission: *January 8, 2014*
- Student Best Presentation Award Application: *January 8, 2014*
- Manuscript Submission: *March 7, 2014*
- Student Travel Award Application: *March 7, 2014*
- Advance Registration: *April 2, 2014*
- Hotel Reservation: *April 23, 2014*

www.intermagconference.com/2014

intermag2014@ifw-dresden.de

IEEE MAGNETICS

Leibniz Institute for Solid State and Materials Research Dresden

CMD Congress Management GmbH Dresden

Tuesday, 06.05.2014

CP - Motors, generators and actuators V 08:00h - 12:00h Terrace foyer Poster

Chair: Wenqiang Chu, University of Sheffield; Kazuo Shima, Kanazawa Institute of Technology

Lihua Zhu	Electromagnetic Vibration Analysis of Motor Core Including Magnetostriction	1
Su-Jin Lee	Equivalent Circuit considering the Harmonics of Core loss in Squirrel-cage Induction Motor for Electrical Power Steering Application	2
Jae-Hoon Jeong	Design Aspects of Exterior Rotor Type BLDC Motor considering permanent magnet overhang for EV/HEV Battery Cooling System	3
Ji-Min Kim	Design of Concentrated Flux Type Ferrite Magnet Motor for Dual Clutch Transmission	4
Alexey Matveev	Permanent magnet generator with three stators for renewable energy converters	5
mi jung kim	Design method and operating characteristics analysis for EV traction induction motor	6
Hanwoong Ahn	Parameter Estimation of Inverter-fed Induction Motor Drives for Direct Vector Control	7
Jing Rao	Electromagnetic Characteristics Analysis of High Speed Traction Motor with Low Switching Frequency Converter	8
Hong Chen	Influence of Rotor Parameters on Performances of Interior Permanent Magnet Machines Applied in Wind Power Generation	9
Yumei Wen	A 3D and wideband vibration energy harvester using magnetoelectric transducer	10
Lin Yang	Design Optimizations of Electromagnetic Devices Using Sensitivity Analysis and Tabu Algorithm	11
S. L. Ho	A Novel Fast Remesh-free Mesh Deformation Method and ItsApplication to Optimal Design of Electromagnetic Devices	12
Jun Cai	Switched Reluctance Position Sensor	13
Ho-Young Lee	The AC Resistance considering Magnetic Saturation Factor in the Motor	14
Guodong Yu	The Effects of Stator and Rotor Eccentricities on Measurement Accuracy of Axial Flux Variable-reluctance Resolver with Sinusoidal Rotor	15
Xianglin Li	A New High-Power-Factor Permanent-Magnet Vernier Machine for Direct-Drive Application	16
Xiu Zhang	A Fast Method to Compute the Torque Curve with Load Angle of Synchronous Machines Using Finite Element Method	17
Zeng Depeng	An Analytical Calculation Model for the Inductances of multi-unit PMSM with Concentrated Windings	18
Longnv Li	A Quantitative Comparative Analysis of Flux-Modulated Electric Motor Using Magnetic Field and Thermal Field Cosimulation	19
Yo Sakaidani	Experimental Verification of Feedback Control of a 2-DOF Spherical Actuator	20

Equivalent Circuit considering the Harmonics of Core loss in the Squirrel cage Induction Motor for Electrical Power Steering Application

Su-Jin Lee, Ji-Min Kim, Dong-Kyun An, Jung-Pyo Hong

Department of Automotive Engineering, Hanyang University, Seoul 133-791, Korea

The consideration of the saturation of the core is essential to the designing of the motor for automotive application, because the size limitations are large in the automotive electric motors, such as those equipped with electrical power steering (EPS). In the design of the squirrel cage induction motor, the equivalent circuit analysis using lumped parameters is often used for investigating the performance of the induction motor. The estimation of the motor characteristics is limited, however, because the standard equivalent circuit considering the space harmonics does not consider the core loss. To improve the reliability of the characteristic analysis, a new method that can solve these problems is required. Thus, the study of a new equivalent circuit that considers the saturation of the core and the harmonics of core loss is needed. Consequently, to obtain the reliable characteristics of the induction motor, this paper presents the modified space harmonic equivalent circuit that considers the harmonics of core loss resistance. The modified equivalent circuit is verified by comparing the analysis results of the suggested method and the experiment results of the test model.

***Index Terms*—Core loss, electrical power steering (EPS), equivalent circuit, harmonics, induction motor.**

I. Introduction

THE induction motor is used in many different fields for operating the small fan to the large automobile engine. Recently, electric vehicles (EVs) and fuel cell electric vehicles (FCEVs) needed various operation regions that make good use of the induction motor [1 - 4].

Electric power steering (EPS) is becoming increasingly favored as the alternative to hydraulic power steering (HPS) because of the advances in electrical machines, sensors, and control electronics. EPS presents several advantages over the conventional HPS, such as improved fuel economy, ability to provide assistance even when the engine is off, and elimination of hydraulic fluid. These benefits result in significant energy savings [5 - 8].

The saturation of the core can not help increasing, because the size limitations are large in the automotive electric motors. Therefore, the consideration of the saturation of the core is essential to designing the motor for automotive application. The most convenient method of analyzing the characteristics in a squirrel cage induction motor is finite element analysis (FEA) [9]. This method, however, requires much computational time and a large memory capacity. In the design of the squirrel cage motor, the equivalent circuit analysis using lumped parameters is often used for investigating the performance of the induction motor [10]. Nevertheless, the estimation of the motor characteristics is limited because the standard equivalent circuit considering the space harmonics does not consider the core loss. To improve the reliability of the characteristic analysis, a new method that can resolve these problems is required. Thus, the study of a new equivalent circuit that considers the saturation of the core and the harmonics of core loss is needed. Consequently, to obtain the reliable characteristics of the induction motor, this paper presents the modified space harmonic equivalent circuit considering the harmonics of core loss resistance.

Manuscript received March 7, 2014. Corresponding author: Jung-Pyo Hong (e-mail: hongjp@hanyang.ac.kr).

Digital Object Identifier inserted by IEEE

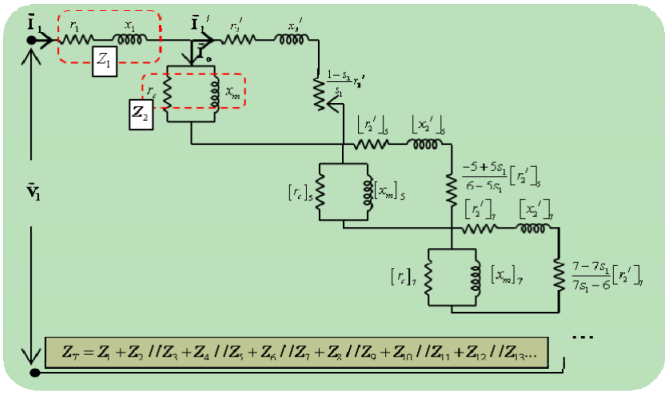

Fig. 1. Modified space harmonic equivalent circuits for the induction motor considering the harmonics core loss.

The relative permeability of the stator and rotor core is renewed by using the *B-H* data from the steel manufacturer. Besides, the magnetic flux distribution is investigated in the load, and then the saturation of the core is considered. The modified equivalent circuit is verified by comparing it with the analysis results of the suggested method and the experiment results of the test model.

II. Modified Equivalent Circuit

A. Conventional equivalent circuit

It has been assumed that the input voltage and current is a sinusoidal wave in the conventional equivalent circuit of the induction motor, but, because the motor that has the teeth-and-slot structure is essentially included in the slot harmonics, as suggested by Alger et al. [10], an equivalent circuit analysis considering the space harmonics is needed. It is occasionally useful to visualize the electromagnetic behavior of the various space harmonics as being similar to the behavior of separate motors, with a common stator winding and a common shaft, but with the magnetizing reactance and secondary impedances corresponding respectively to the air gap flux wave of each specific harmonic. Viewing the various space harmonics from the above point of view is the harmonics torque on the

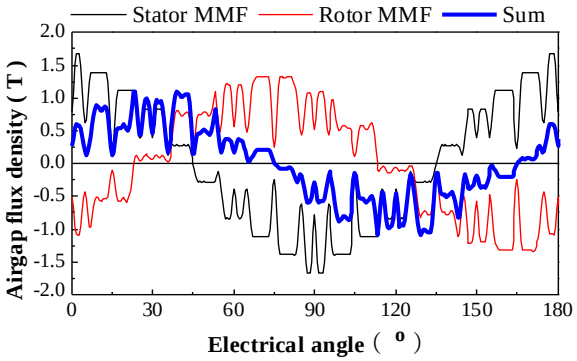

Fig. 2. Air gap flux density by stator and rotor winding

fundamental speed-torque curve. Nevertheless, the estimation of the motor characteristics is limited because the standard equivalent circuit considering the space harmonics does not consider the core loss. To improve the reliability of the characteristic analysis, a new method that can solve these problems is required.

B. Modified equivalent circuit

A modified equivalent circuit is shown in Fig. 1. In this circuit the phase quantities r_1, x_1, r_2', x_2', r_c, and x_m are identical to those used with the standard equivalent circuit. The magnetizing reactance and core loss resistance of each harmonic are based on the component of the air gap flux of that particular harmonic. As the motor with the teeth-and-slot structure is essentially included in the slot harmonics, the flux density in the air gap contains the slot harmonics of the stator and rotor. The air gap flux density by stator and rotor MMF is shown in Fig. 2. The ratio of the area per pole of the k_{th} harmonic to the area per pole of the fundamental wave is *1/k*. Then, as the flux is equal to flux density *B* multiplied by the area per pole, the ratio of the flux per pole for the k_{th} harmonic to the flux per pole of the fundamental is equal to *1/k* times. As the voltage induced in the winding is proportional to the magnetizing reactance, the rotor parameters $[r_2']_k$, and $[x_2']_k$ are based on the impedance of the effective rotor winding.

It will be noted that the slip function of $[r_2']_k$, and $[x_2']_k$ for each harmonic is set up for the rotor slip for that particular harmonic, and is dependent on the order of the harmonic and on whether the harmonic field is forward-rotating (s_k^+) or backward-rotating (s_k^-).

$$s_k^+ = \frac{n_k - n}{n_k} = \frac{\frac{n^s}{k} - n}{\frac{n_s}{k}} = \frac{n_s - kn}{n_s} = 1 - k\left(1 - s_1\right) = (1-k) + ks_1 \quad (1)$$

$$s_k^- = \frac{n_k + n}{n_k} = \frac{\frac{n^s}{k} + n}{\frac{n_s}{k}} = \frac{n_s + kn}{n_s} = 1 + k\left(1 - s_1\right) = (1+k) - ks_1 \quad (2)$$

There will be several harmonic torque dips on the resultant motor torque, and the space harmonics can have a large impact on the induction motor starting. Additionally, to obtain the reliable characteristics of the induction motor, this paper presents the modified space harmonic equivalent circuit considering the harmonics of core loss resistance.

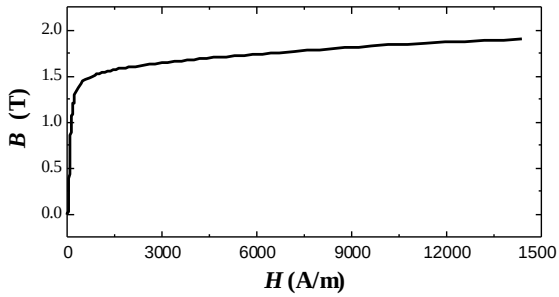

Fig. 3. DC saturation curve of steel

III. Effect of the Saturation of the Core

Fig. 3 shows a plot of the corresponding values of *B* and *H* for magnetic core steel from the steel manufacturer. Such plot gives the familiar normal saturation curve of the material and is of course an important magnetic characteristic of that material.

The reluctance is expressed based solely on geometric data of the motor, the material information, and the winding distributions, as shown in Fig. 4. The single tooth equivalent is calculated by using the tri-diagonal matrix algorithm (TDMA).

The flux density in the core is obtained through single-tooth magnetic circuit analysis considering the nonlinearity of non-oriented silicon steel. At this time, to consider the change of the flux path due to the stator and rotor MMF, the stator and rotor MMFs are inputted respectively. To verify the proposed analysis method, the validity of the analysis results is verified by comparing them with the FEA result. Fig. 5 compares the flux density of the stator teeth using the modified equivalent circuit results with the FEA result under the load condition (@ slip 0.2). It can be seen that the profiles of the flux density distribution by stator and rotor MMF are very close to them. To consider the saturation of the core, this paper introduces the saturation factor (k_{sat}). The saturation factor accounts for sum of the MMF loss in the core and air gap as divided by the MMF loss in the air gap.

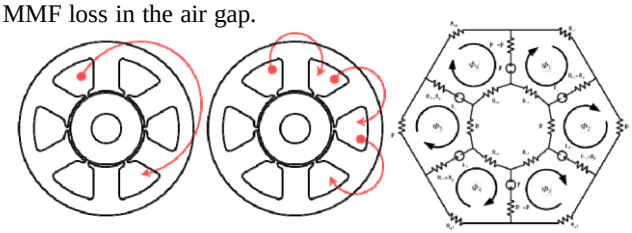

Fig. 4. Concept of the single tooth equivalent

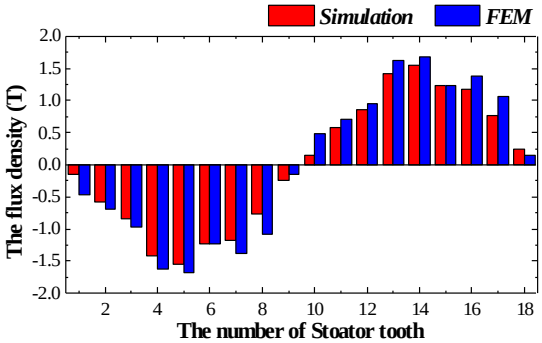

Fig. 5. Distribution of the flux density in the stator teeth @ slip 0.2

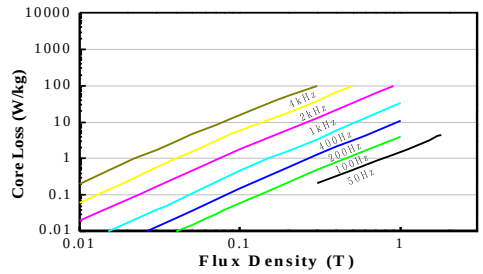

Fig. 6. Core loss data

TABLE I
FUNCTION EXPRESSION OF THE CORE LOSS COEFFICIENTS

Coefficient	Function	A	B
Hysteresis	$A+B/x^{0.5}$	*0.00135*	*0.0144*
Eddy current	$A+B/x^{0.5}$	*0.0000374*	*0.00196*
Anomalous	$A+B/x^{0.5}$	*0.00087*	*0.00742*

Consequently, the presence of a core may be considered an increased air gap g´ [10].

$$k_{sat} = \frac{AT_g + AT_c}{AT_g} \tag{3}$$

where AT_g, and AT_c are the MMF losses of the air gap and the core respectively. The saturation factor was calculated using the iteration routine and the numerical technique.

IV. CALCULATION OF THE HARMONICS CORE LOSS

Motors are becoming more and more favored to the high speed machine due to their high efficiency, miniaturization, and light weight. As a result, the precise prediction of the core loss accounting for a large percentage of the total energy loss in the induction motor is very important for improving the performance capability of the motor under all operating conditions. The three typical models are the empirical formula, FEA, and equivalent circuit models. These models have both strengths and weaknesses. In the case of the empirical formula model, a set of approximation models is used to predict the core loss of the induction motor. This method has been proven to have high precision in predicting the core loss in transformers where the alternating field is dominant. Nevertheless, in rotating machines, in which the flux density variation is very complex, less satisfactory results have been obtained. On the other hand, the FEA makes it possible to consider the rotational core loss as well as the core loss caused by the flux density harmonics in rotating machines, but it is cumbersome and needs much iteration for every operating condition. In the equivalent circuit model, however, if the modeling of the core loss resistance inserted in a parallel way in the circuit is correct, the prediction of the core loss according to the load condition is feasible without a number of iterations, as with the FEA. In this paper, the core loss density considering the excess or anomalous loss is expressed as follows [9] :

$$P_{ck} = P_h + P_e + P_a = k_h f B^n + k_e f^2 B^2 + k_a f^{1.5} B^{1.5} \tag{4}$$

where B is the peak value of the flux density, f *is* the frequency, k_h is the hysteresis loss coefficient, k_e is the eddy current loss coefficient, k_a is the anomalous loss coefficient, n is the Steinmetz constant, and the decision is 2 in this paper.

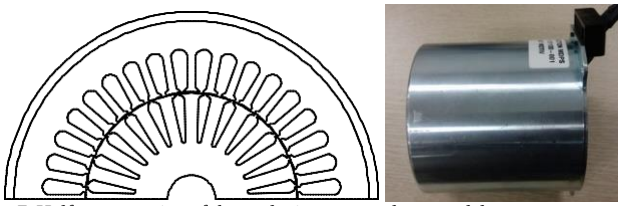

Fig. 7. Half cross-section of the analysis motor and test model

TABLE II
SPECIFICATIONS OF THE MODEL

Item	Unit	Value
Number of poles	-	*4*
Number of the stator slots	-	*36*
Number of the rotor slots	-	*24*
DC link voltage	*V*	*12*
Rated Powers	*W*	*450*
Rated speed	*rpm*	*1500*

Fig. 6 shows the core loss data from the steel manufacturer. As you can be seen, only the data at 50 kHz are given. Therefore, in this paper, the core loss data expressed as the function are obtained as below.

(1) The core loss data provided by the manufacturer are rearranged and plotted as a function of P_{core}/f vs. B.
(2) The frequency vs. core loss data are plotted through the curve fitting of P_{core}/f vs. B.
(3) The derivation of the non-linear curve fitting functions for the core loss coefficients is shown in Table I.

The fundamental core loss and the harmonic core loss are calculated, respectively, using the frequency and the flux density of the core, such as each tooth, yoke, and rotor calculated in section IV. The electromotive force is estimated using the ratio of the k_{th} harmonics content, and then each harmonic core loss resistance is calculated. As a result, in the harmonic equivalent circuit, the core loss resistance is calculated using in (5).

$$[r_c]_k = \frac{E_k^2}{P_{ck}/3} \tag{5}$$

where E_k is the k_{th} back-emf and P_{ck} is the total core loss.

The model was developed based solely on geometric data, material information, and winding distributions. The model takes into account the local saturation of the individual stator and rotor teeth as well as the back yoke sections of the motor.

V. VERIFICATION OF THE HARMONIC EQUIVALENT CIRCUIT

The described models were applied for the analysis of a three-phase, four-pole, and squirrel cage induction motor. The parameters of the machine equivalent circuits were calculated for operation with a fundamental frequency of 50Hz. A cross-section view of the analysis model and the test motor for EPS application is shown in Fig. 7. The detailed specifications of this motor are listed in Table II. Fig. 8 shows the testing apparatus that was used to measure the characteristics of the motor. The comparison of the test and equivalent circuit results is shown in Table III. As previously stated, the conventional equivalent circuit analysis assumed that the input voltage and current are a sinusoidal wave, and the slot harmonics were ignored. Therefore, these results have a big error. As the existing standard equivalent circuit considering

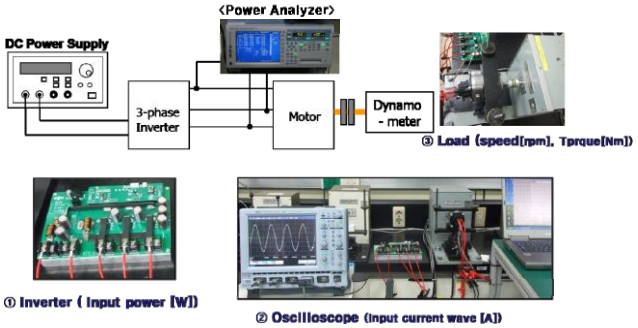

Fig. 8. Testing apparatus for measuring the characteristics

the space harmonics is unconcerned about the core loss, the input current and efficiency, and the power factor, has a bigger error than the modified equivalent circuit.

Fig. 9 compares the conventional and modified equivalent circuit results with the measurement results under the load condition (@ slip 0.2). This figure shows that the conventional equivalent circuit underestimates the space harmonics while the modified equivalent circuit provides more accurate simulation. Additionally, it shows that the standard equivalent circuit considering the space harmonics underestimates the harmonic core loss while the modified equivalent circuit provides more accurate simulation. The obtained results illustrate the proposed model's suitability for nonsinusoidal wave supply analysis considering the harmonic core losses.

VI. Conclusion

To obtain the more reliable characteristics of the induction motor, this paper presents the modified space harmonic equivalent circuit considering the harmonics of core loss resistance and the saturation of the core.

The modified space harmonic equivalent circuit based solely on geometric data, material information, and winding distributions has the following advantages:

(1) The modified harmonic equivalent circuit is accomplished by the proposed approach that improved the estimation of the characteristic in the induction motor compared with the result of the present method. The validation of the analysis result in this paper was verified by this experiment.

(2) The modified harmonic equivalent circuit can quickly present the direction of the initial design. In other words, the proposed method is a technique that can reduce the design time and cost. Thus, the proposed method in the induction motor is very useful for the initial design. Additionally, improvement of the quality and reduction of the cost at the initial design are the expected applications of this study.

Acknowledgment

This research was supported by the MSIP (Ministry of Science, ICT&Future Planning), Korea, under the CITRC (Convergence Information Technology Re-search Center) support program (NIPA-2013-H0401-13-1008) supervised by the NIPA (National IT Industry Promotion Agency).

TABLE III
Comparison of the Test and Equivalent Circuit Results

Item	Test	Convention	Standard Space Harmonic	Modification
Voltage [V_{phase_rms}]	*3.86*	*3.86*	*3.86*	*3.86*
Toque [*Nm*]	*3.66*	*3.43*	*3.72*	*3.69*
Speed [*rpm*]	*1200*	*1200*	*1200*	*1200*
Current [*Arms*]	*74.62*	*76.88*	*72.78*	*73.31*
Out Power [*W*]	*459.9*	*431.1*	*467.0*	*463.5*
Efficiency [*%*]	*60.82*	*58.24*	*61.28*	*59.95*
Power factor [*%*]	*89.74*	*83.10*	*91.48*	*92.14*

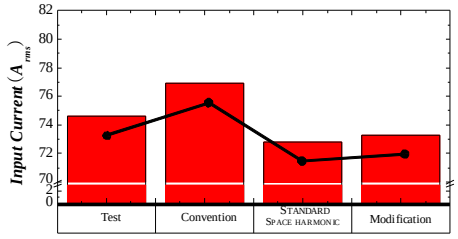

(a) Current spectrum under the load condition

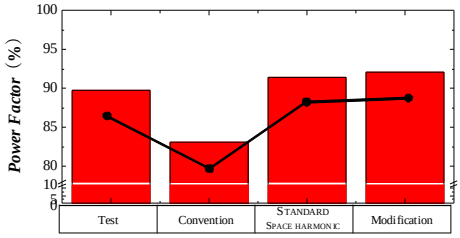

(b) Power factor under the load condition

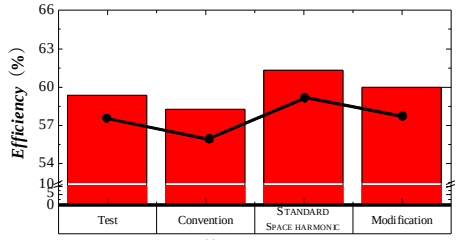

(c) Efficiency under the load condition

Fig. 9. Comparison of the conventional and modified equivalent circuit results with the results of the measurements under the load condition

References

[1] F. Thomas, Finken, H. Kay, "Design of Electric Motors for Hybrid and Electric Vehicle Applications," in *Proc. ICEMS, 2009.*

[2] S. Saliltip, C. Nontawat, "A Samplified Modulation Strategy for Three-leg Voltage Source Inverter Fed Unsymmetrical Two-winding Induction Motor," *J. Electr. Eng. Technol.*, vol. 8, no 6, pp. 1337-1344, Nov. 2013.

[3] F. Khoucha, S. M. Lagoun, K. Marouani, A. Kheloui,"Hybrid Cascaded H-Bridge Multilevel-Inverter Induction-Motor-Drive Direct Torque Control for Automotive Applications," *IEEE Trans. Ind. Electron.*, vol. 57, no 3, pp. 892-2010, Mar. 2010.

[4] S. S. Williamson, A. Emadi, K. Rajashekara, "Comprehensive Efficiency Modeling of Electric Traction Motor Drives for Hybrid Electric Vehicle Propulsion Applications," *IEEE Trans. Magn.*, vol. 56, no 4, pp. 1561-1572, July 2007.

[5] S. Mhamed, K. Hartani, A. Draou, A. Allali, "Sensorless Fuzzy Direct Torque Control for High Performance Electric Vehicle with Four In Wheel Motor," *J. Electr. Eng. Technol.*, vol. 8, no 3, pp. 530-543, 2013.

[6] G. H. Lee, W. C. Choi, S. I. Kim, S. O. Kwon, J. P. Hong, "Torque Ripple Minimization Control of Permanent Magnet Synchronous Motor for EPS application," *Int. J. Automot. Technol.*, 12, (2), pp. 291–297, 2011

[7] S. J. Lee, S. I. Kim, J. P. Hong, "A Study on Characteristics of PM Synchronous Motors According to Pole Slot Combinations for EPS application," *in Proc. Compumag*, 2011

[8] I. Boldea, *The induction machine Handbook*, CRC Press LLC, 2001

[9] L. Cochran Paul, *Polyphase indtuon motor Analysis, Desing, and Application*, Marcel Dekker,Inc, 1989.